Chapter 1

Introduction

Motivation

Diode lasers are the most efficient devices in converting electrical into optical energy and are thus key components for numerous modern technologies. They serve as tools for material processing [Li00, Sch00], are used in optical communications and sensing applications, and are vital elements in medical apparatus [Nas14]. Compared to other established laser systems such as gas, solid state or fibre lasers, the direct electrical pumping of diode lasers enables the construction of robust, simple systems with a small footprint and long lifetimes. The variety of available semiconductor materials allows to choose the diode's wavelength from a broad spectrum. The linewidth can be narrowed to $< 1\,\mathrm{nm}$ by the implementation of gratings [Sch10]. Furthermore, the low cost of diode lasers due to the scalability of the fabrication process makes them commercially appealing. The major disadvantages of high power, high efficiency broad area (BA) diode lasers are their poor beam quality and their low coherence, limiting their use for direct applications in industry. Using them as optical pumps for solid-state and fibre lasers, however, exploits the high powers and efficiencies of the diodes while enabling good beam qualities.

In solid-state laser system with high pulse energies, chirped-pulse amplification (CPA) is widely used to achieve extremely high peak powers. The CPA systems consist of a seed laser whose fs-pulses are temporally stretched (chirped) before being amplified. The resulting ns-pulses can absorb higher pump energies without reaching the damage thresholds of the gain medium, leading to higher amplified pulse energies. After the amplification stages, the pulse is again temporally compressed, so that fs- or ps-pulses with TW-class powers are available [Mas11]. Almost all of the energy in the pulse is thus supplied by the optical power amplifiers, which are made of solid state material and are often cryogenically cooled [Ert11, Fan07]. One common configuration is to use amplifier slabs (e.g. doped YAG crystals) which the laser pulse transverses while being amplified. All the optical energy generated by these amplifiers is provided by optical pumps. The choice of the pumps is often driven by commercial considerations, so flashlamps are commonly used, as they are easily available at a low purchase cost (in \$/W).

One of the most prominent and largest example for a CPA based ultra-high energy class laser facility is located in the National Ignition Facility (NIF) of the Lawrence Livermore Laboratories which is performing studies that seek to achieve nuclear fusion by laser ignition [Mil04]. Figure 1.1 schematically shows NIF's layout in which 192 solid-state lasers are focused onto a target within the reaction chamber. Future fusion power plants based on the findings of NIF will require optical pump powers of $\sim 100\,\mathrm{GW}$ [Der11] for Nd:YAG [Mos11] and Yb:YAG [Mas11.2] solid-state amplifiers. In these power plants, the use of flashlamps as pumps is not feasible, as they require high amounts of maintenance and only achieve low efficiency levels at low pulse repetition rates [Ert11]. To ensure a net power generation and to make the laser induced fusion technology affordable, low cost diode lasers with the highest powers and efficiencies are required.

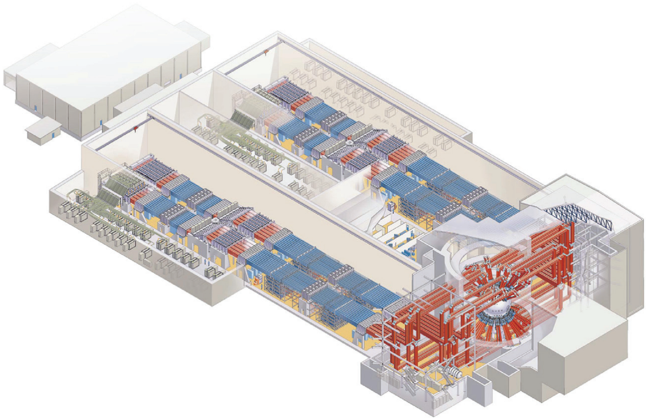

Figure 1.1: Schematic layout of the 192 beamlines and the target chamber at the National Ignition Facility. Figure taken from [NIF16].

Within the *Cryolaser* project[1], the development of these kind of diode laser pump sources was pursued. Specifically, pumps for cryogenically cooled Yb:YAG slabs were targeted, possibly enabling a lower operation temperature of the diode lasers as well. A step size increase in output power and efficiency levels of cryogenically cooled diode lasers is expected to advance their implementation into high energy class laser facilities using solid state laser systems.

State of the art

Power conversion efficiencies of $> 70\%$ have been reported from AlGaAs based, edge-emitting high-power BA lasers operated at room temperature [Kan05, Cru05, Cru13]. Compared to these, commercially available single emitter (SE) BA lasers are usually $w \sim 100\,\mu\mathrm{m}$ wide and emit at wavelengths of $\lambda = 910$-$980\,\mathrm{nm}$ with operation output powers $P \geq 10\,\mathrm{W}$ and efficiencies $\eta_\mathrm{E} \approx 60$-$65\%$ [Lau12]. Output powers of $P = 25\,\mathrm{W}$ have been achieved in continuous wave (CW) mode [Cru09].

[1] funded by the Leibniz Gesellschaft under contract SAW-2012-FBH-2

A few studies have been published on the effects of low-temperature operation on the performance of diode lasers. In [Cru06], the authors report an increase of peak efficiency to 85% in a GaAs-based BA laser operated at $-50\,°C$. Significant benefits to output power and efficiency were further reported for InP-based diode lasers at lower operation temperatures in [Mai08], with increases of up to > + 300% seen in power and + 20% points in efficiency compared to room temperature operation. Record peak conversion efficiencies of 73% have also been published in [Lei10] from InGaAsP-based diode lasers emitting at $\lambda = 1.5\,\mu m$, which were achieved by reducing the operation temperature to 77 K (-196 °C) and using a tailored vertical design.
Electrically operating multiple single emitters on one monolithic piece of semiconductor material in parallel increases the available output power of the component, termed diode laser bar. While such bars have been widely used as quasi-continuous wave (QCW) pump sources for a long time [Die00] and are commercially available with output powers around 300-400 W [Dei08, Ber11, Koh12, Luc15], kW-range bars have also recently been demonstrated, as shown in table 1.1. The chronologically sorted, published results refer to bars with an industrial standard width of 1 cm. It is apparent from the published values in table 1.1, that achievable output powers from a diode laser bar depend heavily on operation conditions (CW / QCW, temperature, ...) and the device's parameters. These parameters will be subsequently discussed for the listed publications and related to the achieved results.
The main difference between CW and QCW operation lies in the amount of dissipated heat in the device, which leads to different cooling requirements. The CW results as well as the early QCW powers of 1.1 kW [Sch07] were achieved from bars mounted on microchannel coolers [Li07, Li08] or similar heatsinks [Kna11] with high heat-removal capacities, while most other publication on QCW bars used simple conduction cooling with lower heat extraction. The need for improved diode lasers to be used as optical pumps is reflected in the higher frequency of publication of QCW bar results starting in 2013 [Kis13, Vet14, Wol14, Che14, Pie15]. Using low duty cycles of $\leq 1\%$, which is the on-time of the laser and is calculated from the pulse width and frequency, the need for expensive and intricate heatsinks with a high heat-removal capacity is avoided and diode laser bars are often integrated into QCW stacked arrays for pumping of solid-state amplifier slabs [Kis13]. The output power of these devices with multiple bars connected in series increases with the number of bars used and represents the need for higher output powers from the optical pumps [Wes13]. While most of the bars were operated at room temperature, a significant increase in output power from 0.7 kW [Li07] to 1 kW [Li08] with an almost constant efficiency is reported which is mainly due to the decreased operation temperature of 8 °C as well as a longer cavity length of $L = 5\,mm$. Wavelength λ and fill factor (FF), which describes the fraction of the 1 cm-wide bar occupied by emitters, are roughly the same. A good overview about impact of the lateral design choice (FF and L) of high power diode laser bars on power and efficiency as well as the underlying economic considerations has been presented in [Cru14]. The exceptionally high powers of 1.8 kW quoted in [Che14] were obtained by using a multi-junction vertical design in which laser structures are epitaxially grown on top of each other, separated by tunnel junctions. While all other cited publications employ single junctions, the use of the three junctions in [Che14] in one bar lead to a strong increase in output power. However, efficiencies are

not given in the publication and are assumed to be lower than for the equivalent use of three single junction bars.

Table 1.1: Published kW-class diode laser bar results with given operation conditions and device parameters.

publication	year	operation	temperature [°C]	λ [nm]	FF [%]	L [mm]	power [kW]	efficiency [%]
[Sch07]	2007	QCW	15	980	44	4	1.1	< 35
[Li07]	2007	CW	25	940	77	3	0.7	58
[Li08]	2008	CW	8	940	83	5	1.0	56
[Kna11]	2011	CW	20	940	77	5	0.94	55
[Kis13]	2013	QCW	20	940	75	1.5	0.71	
[Vet14]	2014	QCW	25	940			0.55	50
[Wol14]	2014	QCW	25	940	75	1.5	0.6	52
[Che14]	2014	QCW	10	870	80	3	1.8	
[Pie15]	2015	QCW	25	940	50	4	0.8	60

No further studies have been published regarding the use of cryogenic operating temperatures for high power single emitters and bars. The benefit of reduced operating temperatures to the output power of bars presented in [Li08] combined with the efficiency increases observed in single emitters at cryogenic temperatures [Cru06] encourages the development of high power, high efficiency diode laser bars for temperatures of 200 K.

Goal of this work

The technical goal of this work is to design high power, high efficiency QCW diode laser bars for peak performance at an operation temperature of $\sim 200\,\mathrm{K}$. This relies on the understanding of the changing semiconductor properties at low temperatures and how they affect the electro-optical properties of the lasers at reduced operation temperature. The temperature dependence of the factors that limit optical output power and power conversion efficiency at high powers needs to be studied and their relative importance has to be assessed. The impact of the vertical and lateral laser design on the performance at lower temperatures has to be analyzed starting on single emitter level. Revised and low temperature optimized vertical designs are sought, which can be fabricated into QCW diode laser bars with the highest output powers and efficiencies.
Specifically, the development and fabrication of exemplary QCW diode laser bars with output powers $> 1.5\,\mathrm{kW}$ and efficiencies $> 60\%$ at this point are targeted, operated at a temperature of $\sim 200\,\mathrm{K}$. Their specifications regarding amongst others wavelength and operation conditions, are governed by their intended use as pump sources for cryogenically cooled Yb:YAG solid state amplifiers and are listed in table 1.2.

Table 1.2: Targeted specifications for low temperature optimized high power, high efficiency QCW diode laser bars.

parameter	symbol	
heatsink temperature	T_{HS}	$\sim 200\,\mathrm{K}$
frequency	f	$10\,\mathrm{Hz}$
pulse length	τ	$1.2\,\mathrm{ms}$
wavelength	λ	$940\,\mathrm{nm}$
bar width		$1\,\mathrm{cm}$
output power	P	$> 1.5\,\mathrm{kW}$
efficiency at P	$\eta_{\mathrm{E}} >$	60%

For economic considerations, the cavity length of the bar should be as short as possible without compromising the power and efficiency levels. Similarly, conduction cooled packaging of the bars instead of microchannel coolers is desired to limit the system complexity. While low spectral width and low vertical beam divergence are potentially beneficial for the pumping of the solid state amplifiers [Ert11], they are not targeted in this work. Wavelength stabilization can be implemented into developed structures at a later stage, for example by surface etched gratings [Fri12].
In order to achieve the high powers levels, the use of high FF ($> 70\%$) in the bars is essential. Assuming a FF $= 75\%$ bar (schematically drawn in figure 1.2) comprised of BA lasers with a usual $w = 100\,\mu\mathrm{m}$ and $L = 4\,\mathrm{mm}$, this represents an output power of $P > 20\,\mathrm{W}$ per single emitter. This estimation does not take into account any deterioration of single emitter performance on bar level due to mounting stress or cross talk between the emitters. However, as long term operation at powers up to $20\,\mathrm{W}$ of single emitters has been demonstrated in CW trials [Cru09], QCW bar operation at the same power level should be feasible.

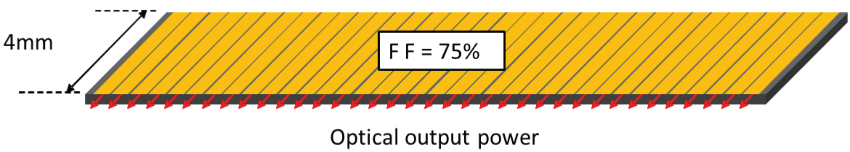

Figure 1.2: Schematic lateral layout of a high fill factor bar.

The work is structured as follows: first, the basic principles of high power, high efficiency diode lasers are explained in chapter 2. The parameters determining optical output power and power conversion efficiency are deduced and their importance for high power, high efficiency operation is estimated. Furthermore, a brief summary of the changes at low temperatures of relevant semiconductor properties is given. In chapter 3, the experimental setup used to characterize the electro-optical performance of single emitters and bars at room temperature as well as lower temperatures is described. The design of a low temperature measurement station and the established accurate power calibration are laid out. Chapter 4 begins with a benchmark assessment of single emitters of different established vertical designs, in which the impact of various vertical design parameters on the electro-optical performance at lower temperatures is studied. High power single emitters and bars of two of the vertical designs are measured and their efficiency-limiting factors are analyzed. In chapter 5, the option of reducing the main efficiency limiting factor, the series resistance, by lowering the Al-content in the waveguide is explored. Low-current measurements are performed on single emitters of epitaxial designs using various Al-contents and insights on the temperature dependence of electrical and optical parameters are gained. Record output powers and efficiencies of fabricated low temperature bars using low Al-content waveguides are presented and options to further increase efficiency at the high powers are discussed. Chapter 6 contains a further approach to reduce series resistance by decreasing the *p*-side waveguide thickness of the vertical structure. Combined with low Al-content waveguides, low temperature optimized epitaxial designs are deduced and experimentally assessed in bar and single emitter format. Finally, all results are summarized and a brief outlook to further improvements is given.

Chapter 2

Theoretical background of high power, high efficiency diode lasers

In this chapter, the basic principles of high power diode lasers are laid out. Diode lasers have been extensively studied and numerous books have been written on the topic. Here, a brief summary of the underlying physics and the properties of the employed materials is given, before diode laser properties and parameters are selectively introduced. The discourse follows the introduction of diode lasers in [Col98] and uses figures from within. No claim for completeness is made as it is out of the scope of this work and the author encourages further reading. Specifically, a comprehensive introduction into solid state physics is given in [Sze01], while the material system of AlGaAs diode lasers is extensively studied in [Ada93]. For additional information on the working principles of diode lasers, [Col98] is recommended, while the device engineering and the fabrication necessary for high power devices is well described in [Die00].
The theoretical background provided in this chapter is limited to topics which are crucial to understand the effects limiting the output power and conversion efficiency in AlGaAs diode lasers. In the first part, the basic working principles of AlGaAs / InGaAs based high power diode lasers are introduced, followed by a discussion of important laser parameters including threshold, output power and power conversion efficiency. Based on a numerical model, the electro-optical performance of a typical single emitter diode laser is simulated and compared for varying characteristic parameters. The second part covers the effect of low temperature operation on the diode laser properties and puts an emphasis on the expected increase of bulk conductivity.

2.1 Basic principles of AlGaAs / InGaAs based diode lasers

Unlike most other laser systems, in which the gain medium has to be optically pumped, diode lasers can be directly pumped by an electrical current, which allows much more efficient operation. Stimulated recombination of carriers between the conduction and valence band of the semiconductor gain medium leads to the emission of photons with energies slightly larger than the band gap. A simple vertical setup of a diode laser is the double-heterostructure which uses a thin layer of undoped active material sandwiched between n- and p-doped cladding layers with a larger band gap. By applying a forward bias, the potential well of the undoped region is filled with injected holes and electrons from the p- and n-side, respectively, and the captured carriers recombine in the active region / zone. The necessary optical feedback for completing a laser is established by cleaved facets of the semiconductor material, which provide a large refractive index step at the semiconductor-air boundary and photons are reflected back into the semiconductor. A transverse dielectric optical waveguide (x direction) is formed by the higher index of refraction in the n- and p-doped cladding layers, so that the light propagates along the plane of the undoped active region (z direction) between the facets for edge emitting diode lasers as schematically drawn in figure 2.1 (a). Separating the optical confinement of photons from the electrical confinement of the carriers in structures termed separate confinement heterostructures (SCH) and using a thin ($d \sim$ 5-10 nm) quantum well (QW) leads to more efficient operation of the diode laser. In figure 2.1 (b), the band gap profiles as well as the electrical field both in transverse direction of such a SCH are shown.

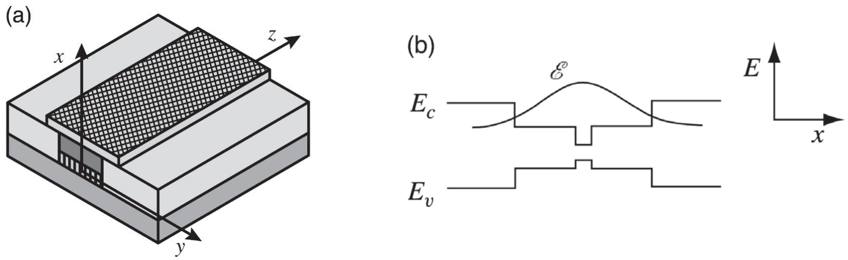

Figure 2.1: (a) Schematic setup of an edge emitting diode laser. (b) Transverse band structures for a standard separate confinement heterostructure. Figures taken from [Col98].

In the structure displayed in figure 2.1 (b), the outer layers (also termed cladding layers) confine the photons to the inner layers (termed waveguides), which in turn provide a confinement for the electrical carriers in the QW. The requirements for the semiconductor materials with different band gaps used to fabricate SCH diode lasers include a common crystal structure and a similar lattice constant for defect-free epitaxial growth of single-crystal layers on top of each other. An exception to the demand for uniform lattice constants is the quantum well. Here, a small lattice mismatch between the QW layer and the surrounding waveguide layers is often desired. The strain in the quantum well causes a separation of the valence band into two bands for light and heavy holes. The former provides optical gain for electromagnetic waves in transversal *magnetic* polarization with the vertical field vector perpendicular to the plane of the QW, while the latter leads to gain for transversal *electric* polarization, in which the vertical field vector is parallel to the QW. Furthermore, lasing threshold and optical loss are reduced in strained layer QWs. Diode lasers in the 0.7-1.6 µm wavelength range most commonly consist of III-V compounds with a direct gap, in which momentum conservation without phonon contribution in the carrier recombination process is satisfied. In figure 2.2, the bandgap of several III-V semiconductors is plotted against the lattice constant. Immediately, the AlGaAs ternary line stands out, as it is almost vertical. This means, that the lattice constant remains approximately unchanged when substituting Al for Ga in GaAs. Thus, a wide range of bandgaps is accessible for designing SCH diode lasers by using layers with different $Al_xGa_{1-x}As$ compositions. For diode lasers in the 9xx nm wavelength range, InGaAs is used as a material for the strained QWs.

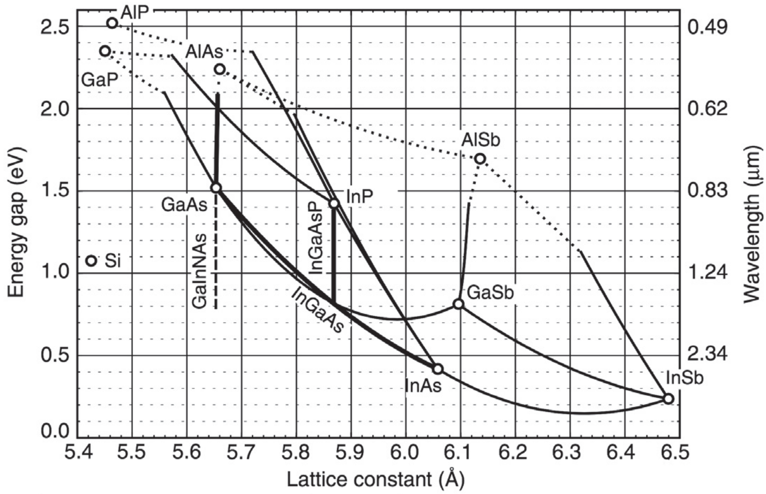

Figure 2.2: Bandgap energy plotted against lattice constant for III-V semiconductors. The single points are binary compounds, with the curves representing ternary compounds with direct (solid) and indirect (dashed) bandgaps. Figure taken from [Col98].

The deposition of the multiple single-crystal lattice-matched layers is achieved by epitaxial growth over a suitable substrate. For edge emitting lasers, the most common deposition techniques are the metal-organic chemical vapor deposition (MOCVD) and molecular beam epitaxy (MBE). While MOCVD growth can remove surface damages of the substrate and offers high quality interfaces between the different layers, MBE excels in film uniformity and well defined thicknesses. For the diode lasers discussed in this work, $Al_xGa_{1-x}As$ layers for the cladding and waveguide layers are deposited by MOCVD on GaAs substrates, with the gain provided by one or multiple strained InGaAs QWs.
After the epitaxial growth, the wafer with the vertical laser structure is laterally patterned to provide lateral optical and current confinement. In this wafer process, the current's path is restricted for edge-emitting diode lasers by applying narrow metallized contact stripes to the top-side (p-side) of the grown structure. Together with insulating layers, selective etching and / or implantation insolation of p-regions, this limits the lateral

carrier distribution on the vertical path through the device. In turn, the creation of photons is also laterally confined to the areas accessible by the current. Possible further implementation of lateral index steps provides boundaries for the extent of the optical field guiding the photons along the axis of the cavity. For common high power broad area lasers (BAL) which are discussed in this work, current is limited to a stripe of w = 70-200 µm width. A typical BAL single emitter with its dimension is displayed in figure 2.3.
After the lateral wafer process, diode bars containing single emitters are cleaved from the wafer with determined cavity lengths. The facet are cleaned, passivated and coated to reflect the light back into the cavity (rear facet with high reflectivity R_r) and transmit the optical output (front facet with anti reflection coating R_f). Finally, single emitters are cleaved from the bar and mounted to expansion matched CuW heatsinks, establishing electrical connections and providing efficient heat removal.

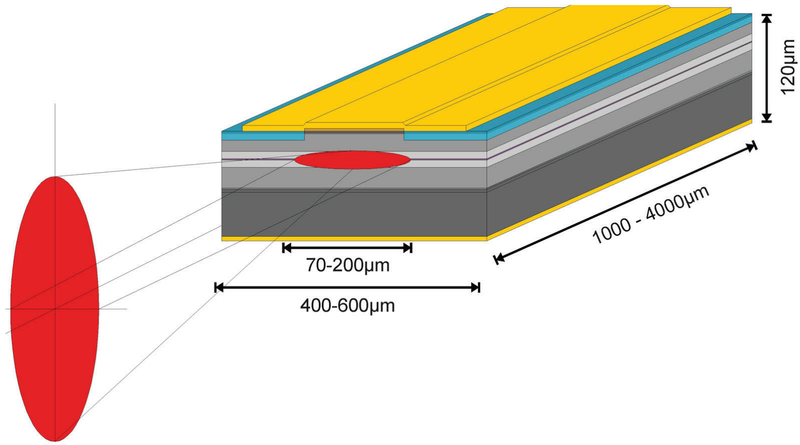

Figure 2.3: Schematics and dimensions of a high power single emitter broad area laser.

2.1.1 Lasing threshold

The conditions at the onset of lasing, namely the threshold gain and the threshold current, are subsequently derived for edge emitting Fabry-Perot (FP) diode lasers. The propagating optical wave along the laser's cavity is described by a normalized transverse field profile $U(x,y)$ established by the dielectric waveguide and its propagation can be expressed by $\exp(-i\beta z)$ with β being the complex propagation constant. For the time- and space-dependent electrical field, polarized in TE (y) direction, this leads to

$$\vec{E}(x,y,z) = E_0 \cdot U(x,y) \exp\left(i\left(\omega t - \beta z\right)\right)\vec{e}_y \tag{2.1}$$

with E_0 being the field's magnitude. β can be expressed as a function of wavelength λ, the transverse modal gain Γg_mod and loss α_i and the effective index of refraction for the mode n_eff